Sensors and Materials, Vol. 9, No. 3 (1997) 131–139
MYU Tokyo

S & M 0279

A Strontium Titanate Thermocapacitive Floating Gate MOS Flow Sensor

Kwang Ming Lin, CheeYee Kwok and Ruey Shing Huang[1]

School of Electrical Engineering, The University of New South Wales,
Sydney, NSW 2052, Australia
[1]Department of Electrical Engineering, National Tsing Hua University, Hsinchu, Taiwan

(Received November 24, 1995; accepted December 24, 1996)

Key words: flow sensor, strontium titanate, floating gate MOS

A new thermocapacitive integrated flow sensor that uses a floating gate MOS transistor has been fabricated. Perovskite strontium titanate ($SrTiO_3$) is used as a dielectric material between the top (control) gate and the floating gate. The temperature dependence of the dielectric constant is about 2000 ppm/°C. The process flow is compatible with standard MOS processes and augmented to include a new capacitor module and bulk micromachining at the final step. The output drain voltage change at a flow velocity of 26 m/s is about 57 mV. Sensitivity in the linear range is 5.5 mV $(m/s)^{-1}$.

1. Introduction

Currently, there is growing demand for high-performance mass flow sensors, notably in the IC industry. Mass flow measurement based on dynamic pressure or friction loss requires very sensitive differential pressure sensors. Direct measurement of mass flow could be made via Coriolis or gyroscopic forces; however, this would require even more sensitive sensors as well as complicated mechanical structures. A better and more common option for the measurement of mass flow is to make use of the ability of the gas to transport heat by forced convection. The advantages of integrated silicon gas flow sensors include low cost arising from batch fabrication, on-chip electronic signal conditioning circuitry for enhanced performance, low power consumption and reduced dimensions. Most of the present integrated silicon flow sensors utilize either thermopile elements, thermoresistive elements or microresonator structure to detect flow. Integrated thermopiles measure temperature changes due to forced convection by gas flow, by means of the Seebeck effect.(1) Thermoresistive flow sensors measure the change in resistance of a thin-film resistor when it is cooled due to forced convection by gas flow.(2) The change in resistance of the sensing resistor is monitored by means of the Wheatstone bridge configuration. As for the microresonator structure,(3) the resonance frequency shift of the microbridge with temperature is used to measure gas flow.

In this paper, we present a new flow sensor which is based upon the thermocapacitive property of a dielectric material. $SrTiO_3$, belonging to the perovskite family, is a dielectric that has sufficiently low leakage current and high temperature-dependent dielectric constant.(4) The $SrTiO_3$ capacitor is incorporated into a floating gate MOS structure such that changes in the dielectric properties due to temperature variations with gas flow would be reflected in the drain current changes.

2. Principle of Operation

The principle of operation of the flow sensor can be best described by the behavior of the floating gate MOS transistor, which is widely used in nonvolatile semiconductor memory such as EPROM and EEPROM,(5) in neuron MOS(6) and in other analog applications such as multipliers.(7) The floating gate potential of the device in Fig. 1, which controls the drain current in the MOSFET based on the usual square-law relationship, is determined via the capacitive coupling of voltages from the input gate (control), drain, source, channel and substrate. When seen from the input gate, the simplified drain current is given by the following relationship: $I_d = (1/2)\ \mathrm{K}\ [w_iV_i + w_bV_b - w(V_s - V_{th})]^2$, where $w_i = C_s/C_T$, $w_b = C_b/C_T$, and $w = (2/3)\ C_{ox}/C_T$ are the coupling ratios associated with the input voltage V_i, substrate potential V_b, and source potential V_s and threshold voltage V_{th}, respectively. K is the transconductance term in which the aspect ratio is included. C_s, which is the sensing capacitance whose dielectric material is $SrTiO_3$, is the coupling

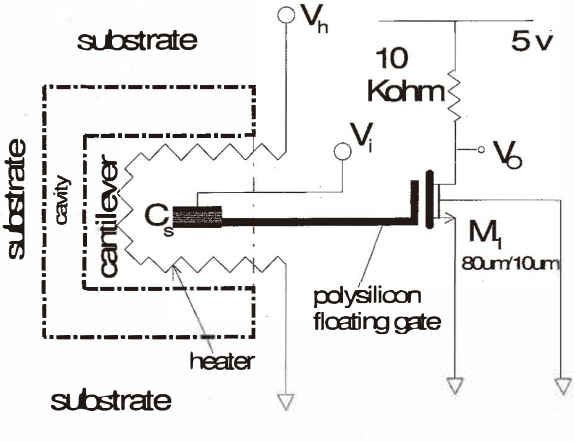

Fig. 1. Schematic of flow sensor circuit.

capacitance between the input gate and the floating gate. C_b is the parasitic coupling capacitance between the floating gate and the well or the substrate. C_{ox} is the gate oxide capacitance of the MOS transistor. C_T is the total capacitance associated with the floating gate and is given by $C_T = C_S + C_b + (2/3)\ C_{ox}$. Source/drain overlap capacitances have been neglected which explains why the drain voltage does not appear in the above drain current equation.

The concept of the floating gate microsensor stems from the observation that for fixed input voltages, the drain current can be modulated by changes in the coupling capacitance C_s between the input gate and the floating gate, which predominantly affect the coupling ratio w_i . However, the other coupling ratios w_b and w are also dependent on C_s through C_T. By taking the derivative of I_d with respect to C_s, it can be shown that the sensitivity of I_d to changes in C_s is given as follows: $S = (C_s\ /\ I_d) \cdot (dI_d\ /\ dC_s) = 2w_i\ [\sqrt{I_d^*/I_d} - 1]$, where I_d^* is the drain current if V_i is applied directly to the floating gate instead of the input gate. The $SrTiO_3$ dielectric in the sensing capacitor C_s has a strong temperature-dependent dielectric constant, typically about 2000 ppm/°C, and a reasonably low leakage current, if deposited under certain conditions and operated at low voltages. For purposes of thermal isolation, the sensing capacitor is located on a cantilever plate obtained by bulk micromachining in EDP anisotropic etchant. The bottom plate of the $SrTiO_3$ sensing capacitor is n^+-doped polysilicon which is an integral part of the floating gate of the MOS transistor M1. The MOS transistor is located on the substrate surface to avoid heat transfer from the heating resistor. When power is applied to the heating resistor, a rise in temperature increases the sensing capacitance C_s which, in turn increases the voltage coupled to the floating gate and causes the drain current to increase. With gas flow, convective cooling on the surface of the capacitor would reduce the capacitance and lower the voltage coupled to the floating gate. Drain current would then decrease. The change in the drain output voltage is therefore a measure of the gas flow rate.

3. Sensor Fabrication

The sensor fabrication process flow begins with the standard MOS process which is modified at the later stages to incorporate the sensing capacitor structure located on a micromachined cantilever structure. The main fabrication steps are illustrated in Fig. 2. The starting material is 8–15 Ω-cm <100> orientation p-type silicon wafer. An oxide layer of 6000 Å thickness is initially grown and patterned to define the channel stop and cantilever areas for boron diffusion. High boron concentration in the cantilever region serves as an etch-stop during bulk micromachining. The oxide layer is removed and a field oxide layer grown. This is followed by definition of the active region for the MOS transistor and, at the same time, the areas surrounding the region for bulk micromachining of the cantilever. After threshold voltage adjustment by implantation, gate oxide of 500 Å thickness is grown, followed by deposition of 4500-Å-thick polysilicon layer. The polysilicon layer constitutes the floating gate of the MOS transistor and extends over the field oxide layer to the cantilever region to form the bottom electrode of the sensing capacitor. The heating element is also formed from this layer of polysilicon. The

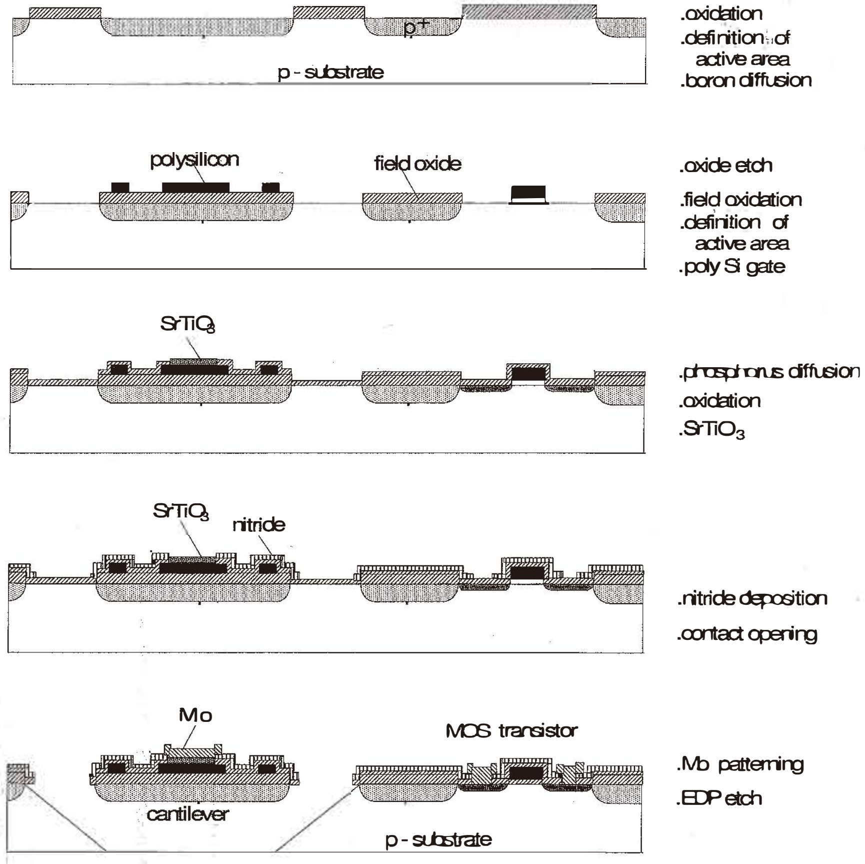

Fig. 2. Illustration of the main fabrication steps.

polysilicon layer is patterned and plasma-etched. The thin oxide layer on the active region is then etched and phosphorus is diffused to form the drain and source regions while the polysilicon layer is doped. This is followed by oxide regrowth. The subsequent steps describe the formation of the sensing capacitor. Unlike other thin-film materials, plasma etching of $SrTiO_3$ films with the desired selectivity is difficult. Hence, the lift-off technique is employed. The oxide layer over the polysilicon layer in the cantilever region where the capacitor is to be formed is patterned and wet-etched. Then 2000-Å-thick $SrTiO_3$ is deposited over the capacitor area by rf sputtering (13.56 MHz, 100 W) followed by resist removal to facilitate lift-off. During the lift-off process, the substrate temperature is kept at room temperature. Deposition rate is 600 Å/h. For the sputtering of $SrTiO_3$, the choice of sputtering gas is critical to achieving good thin-film electrical characteristics. The films are sputtered in 40 Pa of O_2 rather than Ar for better electrical characterisitics.(4)

In order to protect the substrate and active device areas from EDP etching, 1500-Å-thick LPCVD silicon nitride is deposited. The nitride is patterned and plasma-etched to form contact openings to the active device and to define the surrounding areas adjacent to the cantilever region. The photoresist used in nitride patterning is removed by O_2 plasma dry etching because sulfuric acid, which is often used in photoresist removal, attacks $SrTiO_3$. Since Mo is not attacked by EDP, it is used as the metallization material. However, in order to achieve good ohmic contact,(8) Al is first evaporated, annealed and removed to facilitate good alloying with silicon at the contact openings. Then Mo is sputtered and patterned. The final processing step is bulk micromachining in EDP at 90°C. The exposed silicon in the region surrounding the three sides of the sensing capacitor facilitates anisotropic etching that would eventually result in the formation of a 160 μm by 160 μm cantilever structure upon which the sensing capacitor is formed. The sensing capacitor dimensions are 28 μm by 100 μm. Figure 3 is an SEM micrograph of the flow sensor, viewed at an angle, showing the sensing capacitor located on the right-hand side of the cantilever structure.

4. Results and Discussion

The sputtering conditions are critical to achieving $SrTiO_3$ film with low leakage current. Oxygen is used as the sputtering gas. Since oxygen tends to be negatively charged in a plasma ambient because of its electron affinity (Ar is positively charged), typical processing pressures of 0.5–2 Pa cannot be used. When typical processing pressures were

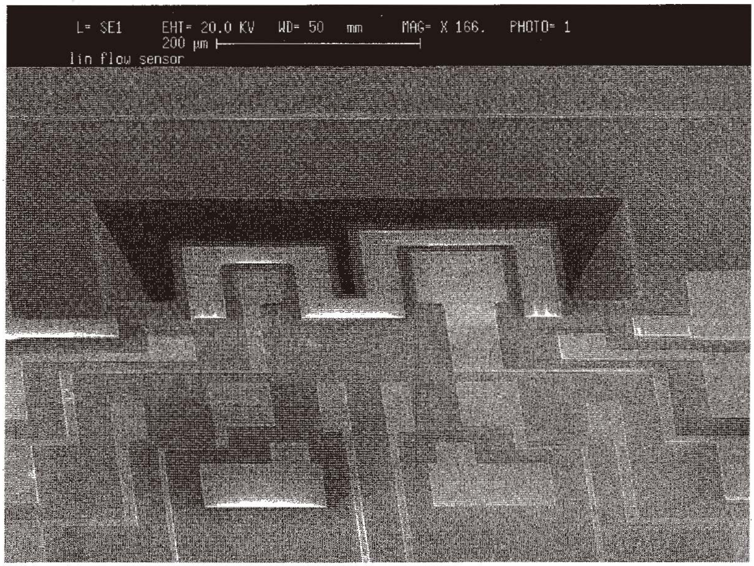

Fig. 3. SEM micrograph of the thermocapacitive flow sensor.

used, not only was $SrTiO_3$ thin film not sputtered onto the wafer but the wafer was also bombarded by O^- species. Furthermore, in view of the lift-off technique employed here, the photoresist patterned on the wafer plays the role of a sputtering mask. Hence, the sputtering gas (oxygen) also etched the photoresist. Thus process conditions must be carefully selected in order to minimize wafer bombardment and photoresist etching. An O_2 operating pressure of 40 Pa was chosen to prevent oxygen deficiency, thereby ensuring good electrical characteristics and reducing the resputtering of the wafer by O^- species due to the increased scattering effect.

$SrTiO_3$ has a cubic crystal structure at room temperature and above.(9) From reports of studies on single-crystal (bulk) $SrTiO_3$, the crystal structure becomes tetragonal at 110 K and orthorhombic at 65 K. The Curie temperature is about 35 K and above which, the dielectric constant temperature dependence varies according to the Curie-Weiss law. At room temperature, the dielectric constant of <001> oriented $SrTiO_3$ crystal is about 330. $SrTiO_3$ is paraelectric at room temperature and exhibits incipient ferroelectricity at very low temperatures.(10) Pyroelectricity in crystals requires them to be non-centrosymmetric and to have a polar axis along which spontaneous polarization exists.(11) Only 10 of the possible 32 point group crystal classes satisfy this condition and the cubic crystal structure of $SrTiO_3$ is not among them.

In view of its high dielectric constant, $SrTiO_3$ thin film has been considered as a candidate for the dielectric material of DRAM capacitors. The dielectric constant of rf-sputtered $SrTiO_3$ films on silicon substrate is lower than that of bulk and depends on substrate temperature during sputtering,(4,12,13) stoichiometry(14) and post-deposition annealing conditions.(15) For silicon substrate temperatures ranging from 200°C to 550°C, the dielectric constant of sputtered $SrTiO_3$ films can range from 30 to 240.(12,13) The dielectric constant dependence on film thickness is explained by the presence of a thin amorphous layer of $SrTiO_3$ and a thin SiO_2 layer of about 100 Å sandwiched between the substrate and the polycrystalline $SrTiO_3$ layer,(16) which can be attributed to the substrate temperature and oxygen ambient during rf sputtering.

CV measurements of the $SrTiO_3$ capacitor test structure gave a dielectric constant of about 40, a temperature-dependent dielectric constant of about 2000 ppm/°C up to a temperature of 110°C and a leakage current of 8×10^{-10} A/cm^2 at 1 V. The low dielectric constant and positive temperature coefficient reported here are consistent with the results of Miyasaka and Matsubara,(13) where sputtering was conducted at low substrate temperatures. The packaged sensor was used to measure nitrogen flow in conjunction with a calibrated flowmeter in which nitrogen gas was used. With only 1 V applied to the input gate, the device was operated in the saturation region and had a drain current of 200 mA. The voltage drop was less than 0.5 V across the sensing capacitor C_s to ensure minimum leakage current. Figure 4 shows the output drain voltage change versus heating power with no gas flow. As the power increases, the ambient temperature of the $SrTiO_3$ sensing capacitor increases which couples more of the input voltage onto the floating gate and lowers the output drain voltage. When gas flow occurs, convective cooling reduces the capacitor temperature, which in turn reduces the voltage coupled to the floating gate. Hence, the output drain voltage increases. With no gas flow, the dc output drain voltage is about 3.0 V. The output drain voltage change ΔV_0 versus gas flow velocity is plotted in Fig. 5

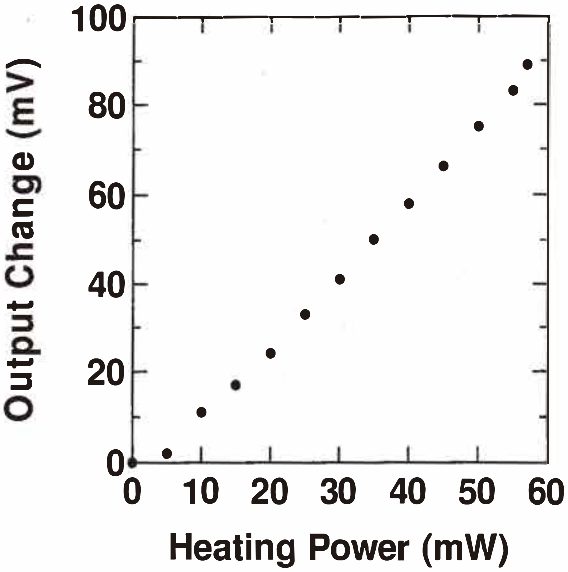

Fig. 4. Output drain voltage change (mV) versus heating power (mW) with no gas flow.

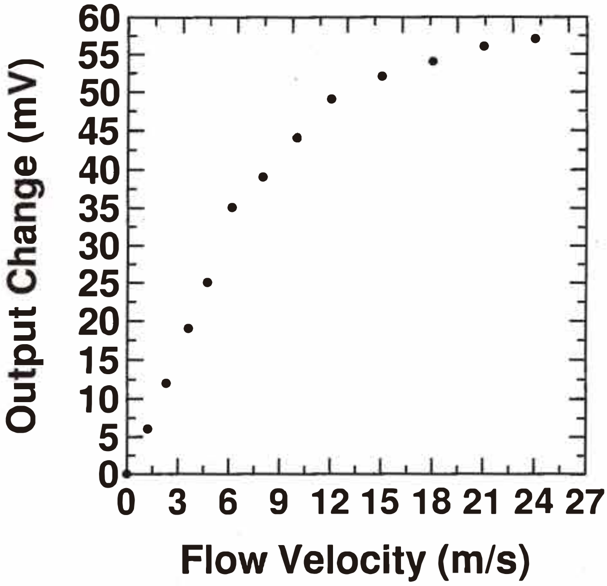

Fig. 5. Output drain voltage change (ΔV_0) in mV versus flow velocity of N_2.

where 57 mW of heater input power was applied. The output characteristics of the flow sensor in Fig. 5 behaved in a manner similar to theoretical models(17) in which assumptions of turbulent gas flow, a velocity boundary layer much thinner than the thermal layer and a constant velocity profile within the thermal boundary layer were made. The output drain voltage change is linear in the range of 0 – 6 m/s and above this value, it saturates at about 57 mV at 26 m/s. The sensitivity in the linear range is 5.5 mV $(m/s)^{-1}$. The response time of the flow sensor is of the order of tens of seconds. This is not surprising when the size of the sensing capacitor used in this prototype is taken into consideration. The dc drift with time of the output drain voltage, which could be attributed to the leakage curent, was monitored over a period of 16 h. The change in the dc output drain voltage was 30 mV over the first 12 h after which it stabilized. The zero-flow dc output drain voltage needs to be measured before flow measurements are made. Over the period of measurement, the output signal change is about two orders of magnitude larger than that due to drift. Further work needs to be done in reducing the drift. Measurements of the MOS transistor current-voltage characteristics and threshold voltage showed no difference, with and without power applied to the heating element, indicating good thermal isolation of the heating element from the rest of the active device. With heating voltage applied to only one terminal of the heating resistor (no current flow), no change in the drain current was observed, which means negligible coupling of the heater potential to the floating gate.

5. Conclusion

An integrated $SrTiO_3$ thermocapacitive floating gate MOS flow sensor has been designed and fabricated. Perovskite $SrTiO_3$ thin film is the dielectric material of choice for the sensing capacitor, which is formed by rf sputtering in O_2 followed by the lift-off technique. The process is compatible with most standard MOS processes. With a temperature-dependent dielectric constant of 2000 ppm/°C, an output signal sensitivity of 5.5 mV/(m/s) in the linear range has been achieved at an input power of 57 mW.

Acknowledgement

The authors wish to thank the staff of the Microelectronics Laboratory and Drs. M. Gross and T. Puzzer of the Plasma Laboratory for their technical assistance, and ARC for the financial support.

References

1 D. Moser, R. Lenggenhager and H. Baltes: Sensors and Actuators **A25–27** (1991) 577.
2 R. G. Johnson and R. E. Higashi: Sensors and Actuators A**11** (1987) 63.
3 S. Bouwstra, R. Legtenberg, H. Tilmaus and M. Elwenspoek: Sensors and Actuators **A21–23** (1990) 332.
4 T. Kuriowa and T. Honda: Jpn. J. Appl. Phys. **31** (1992) 3025.
5 A. Kolodny, S. T. K. Nieh, B. Eitan and J. Shappir: IEEE, Trans. Electron Devices **ED–33** (1986) 835.

6 T. Shibata and T. Ohmi: IEEE, Trans. Electron Devices **ED–40** (1993) 570.
7 H. R. Merhvarz and C. Y. Kwok: IEEE ISSCC'95 Technical Digest (San Francisco, 1995) 60.
8 KM. Lin, C. Y. Kwok and R. S. Huang: J. Micromechanics and Microengineering **6** (1996) 236.
9 R. C. Neville, B. Hoeneisen and C. A. Mead: J. Appl. Phys. **43** (1972) 2124.
10 M. E. Lines and A. M. Glass: Principles and Applications of Ferroelectrics and Related Materials (Oxford, 1979) 225.
11 S. T. Liu: LANDOLT–BÖRNSTEIN, (Ed. K. H. Hellwege), Group III, 11 (1979) 471.
12 W. B. Pennebaker: IBM J. Res. Dev. **13** (1969) 686.
13 Y. Miyasaka and S. Matsubara: IEEE, Proc. 7th ISAF (1990) 121.
14 T. Hirano, M. Taga and T. Kobayashi: Jpn. J. Appl. Phys. **32** (1993) L1760.
15 S. Otani, M. Kimura and N Sasaki: Appl. Phys. Lett. **63** (1993) 1889.
16 S. Matsubara, T. Sakuma, S. Yamamichi, H. Yamaguchi and Y. Miyasaka: Mat. Res. Soc. Symp. **200** (1990) 243.
17 G. Wachutka, R. Lenggenhager, D. Moser and H. Baltes: Technical Digest, IEEE Transducer '91 (San Francisco, 1991) 22.